

## XRD PROFILE ANALYSIS OF INTERCALATED MONTMORILLONITES

DANIEL JANEBA<sup>1</sup>, PAVLA ČAPKOVÁ<sup>1</sup> and ZDENĚK WEISS<sup>2</sup>

<sup>1</sup>Faculty of Mathematics and Physics, Charles University, Ke Karlovu 3, 121 16 Prague 2, Czech Republic

<sup>2</sup>Central Analytical Laboratory, Technical University of Mining and Metallurgy, 708 33 Ostrava, Czech Republic

(Manuscript received October 14, 1996; accepted in revised form January 7, 1997)

**Abstract:** X-ray diffraction analysis of natural and intercalated montmorillonites is usually limited to the apparent d-spacings estimated from the peak maxima in the raw data. This can lead to different estimated d-spacings and to the wrong interpretation of the measured data. In the case of X-ray diffraction, the interference function is modulated by instrumental and physical factors which lead to distortions of diffraction profiles and to the shift of the peak position. The present work deals with the detailed analysis of these effects, their corrections and their consequences for the interpretation of diffraction patterns. On the example of montmorillonite intercalated with Al-hydroxy polymers, it is shown that the difference between the d-spacing estimated from raw data and the d-spacing after the correction for angular dependent factors is about 1 Å.

**Key words:** montmorillonite, intercalation, XRD, profile analysis.

### Introduction

The technology of PILC (pillared clays) synthesis requires careful monitoring based on the accurate and reliable analysis of prepared material. X-ray diffraction analysis of original and pillared montmorillonites, presented in literature is almost limited to the apparent d-spacings estimated from the peak maxima in the raw data. This leads to different observed values of d-spacings which are presented in the literature. The reason for these differences is not only the different deposit of montmorillonites but also measurement influences. For structures exhibiting the diffraction line broadening, the low angle region of diffraction pattern shows certain characteristic distortions arising from instrumental factors (Lorentz-polarization factor, diffraction geometry) and physical factors (structure factor — Reynolds 1980, 1989, surface roughness effect) as a continuous function of diffraction angle, regardless of the cause of the line broadening. The present work deals with the detailed analysis of these effects and their consequences for interpretation of diffraction patterns (i.e. the incorrect determination of lattice parameters and possible incorrect conclusions concerning structural disorder and the phase identification). The way to get the true d-spacings of basal planes of the montmorillonite structure (i.e. determination of the lattice parameter  $c$ ) is shown in this paper together with the possibility of getting some more information about the interlayer structure (i.e. to find any

indices for the presence of certain types of cation). This profile analysis can also lead to determination of the phase composition of intercalated montmorillonite (i.e. to distinguish between the interstratified structure with irregular mixing of two d-spacings values corresponding to the intercalated and the nonintercalated montmorillonite and mixture of two segregated phases intercalated and nonintercalated).

### Theory

Turbostratic arrangement of silicate layers in certain clay minerals, notably in those of the smectite group, strongly affects the diffraction pattern. Consequently the powder diffraction pattern shows mainly basal (001) reflections and two-dimensional  $hk$  diffraction bands. These  $hk$  bands are not well suited to structure analysis and the identification and description is mainly based on the basal reflections. The distortion of silicate layers, small particle size and irregular mixing of different basal spacings in the layer stacking, lead to the (001) line broadening. Moreover the intensities are reduced by thermal motion. As a result of all these effects, only 2–3 basal reflections are usually observable and consequently the information content of diffraction pattern is very limited in the case of smectite. The present work deals with the profile analysis of the (001) serie.

The integral and profile intensity (in case of powder sample) is given (Klug & Alexander 1974) by the formula:

$$I_{hkl} = S \cdot L_p \cdot F_{hkl}^2 \cdot A$$

$$I(2\Theta) = S \cdot L_p \cdot F^2(2\Theta) \cdot A \cdot \Phi$$

where

$S$  is scale,

$L_p$  is Lorentz polarization factor,

$F^2$  is structure factor,

$A$  is absorption,

$\Phi$  is profile function.

In the case of narrow diffraction lines we can assume that the angular dependent terms ( $L_p$ ,  $F^2$ ,  $A$ ) do not change across the line width and therefore the line position can be taken as the position of maximum intensity. The situation with broadened lines is different (see Reynolds). If the diffraction profiles are broadened, the angle dependence of these factors has to be taken into account. The considerable change of the line profiles and consequently the shift of the peak maxima to lower  $2\Theta$  angle have been observed after the correction of experimental diffraction diagrams for these angle dependent factors ( $L_p$ ,  $F^2$ ,  $A$ ). These changes stimulated us to a more detailed investigation of these effects.

### 1. Lorentz-polarization factor

The Lorentz-polarization factor for Bragg-Brentano geometry (without monochromator) is given:

$$L_p = \frac{1 + \cos^2 2\theta}{2 \sin^2 \theta \cos \theta}$$

### 2. The absorption

a) The volume absorption for symmetrical Bragg-Brentano geometry ( $\alpha = \beta = \Theta$ ,  $\alpha$ ,  $\beta$  are the angles between the sample surface and the incident and diffracted beam) and thick sample ( $t \rightarrow \infty$ ) is

$$A = \frac{1}{2\mu}$$

where  $\mu$  is the absorption coefficient. Therefore this kind of absorption can be assumed to be angular independent and does not contribute to the angular dependent corrections.

### b) Surface roughness effect

There is a strong absorption on the rough surface. If the surface is modeled as a surface with cubes upon it (see Fig. 1), the radiation has to pass the cube before reaching the detector. Then the intensity (Berg & Wachtters) is

$$I(\alpha, \beta) = I(90^\circ, 90^\circ) [1 - \varepsilon(\cot \alpha + \cot \beta)]$$

$$\varepsilon = Nd^2 [1 - \exp(-\mu d)]$$

where

$N$  is the number of cubes per unit area

$d$  is the edge of the cube

$\alpha, \beta \leq 90^\circ$ ,  $\alpha + \beta = 2\Theta$

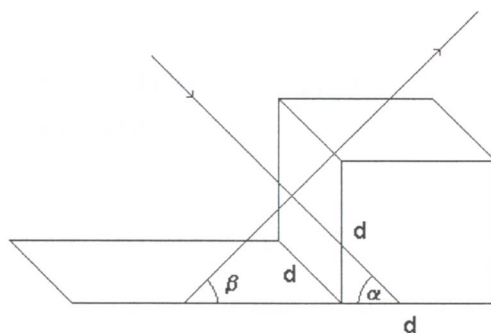


Fig. 1. Surface roughness effect.

For an ideal rough surface half of the surface area is covered by cubes. With symmetrical Bragg-Brentano geometry ( $\alpha = \beta = \Theta$ ) and the cube edge  $5 \cdot 10^{-6}$  m this gives the dependence:

$$I_{BB} = 1 - \cot \Theta$$

### 3. The structure factor

The angular dependency of the structure factor is given by

$$F(2\theta) = \sum_{j=1}^N n_j f_j \left( \frac{\sin \theta}{\lambda} \right) \cos \left( \frac{4\pi z_j \sin \theta}{\lambda} \right) + i \sum_{j=1}^N n_j f_j \sin \left( \frac{4\pi z_j \sin \theta}{\lambda} \right)$$

where

$n_j$  is number of atoms of each type in unit cell in positions  $z_j$  (in Angstroms)

$f_j$  is atomic scattering amplitudes (from ITC):

$$f \left( \frac{\sin \theta}{\lambda} \right) = \sum_{i=1}^4 a_i \exp \left[ -b_i \left( \frac{\sin \theta}{\lambda} \right)^2 \right] + c$$

## Experimental

X-ray powder diffraction diagrams were obtained with a Philips powder diffractometer — vertical goniometer, using the wavelength  $\text{CuK}\alpha$  (Ni filter). The step size  $0.02^\circ$  in  $2\Theta$  and measuring time 20 sec per step have been used for the diffraction pattern recording. The divergence slit was  $1/6^\circ$ , scatter slit  $0.1 \times 10^{-3}$  m, receiving slit  $0.1 \times 10^{-3}$  m. The radius of the goniometer was 0.17 m.

As the flat sample holder is in the horizontal position during the measurement, powder can be pressed into the sample holder without any binding agent. The samples prepared by this method obviously showed the 001 preferred orientation.

The natural Na-MMT was intercalated in aqueous solution where  $\text{Na}^+$  ions were replaced by Al-hydroxy complexes. The intercalated sample contained 25 % of Na-MMT matrix (which follows from the chemical analysis).



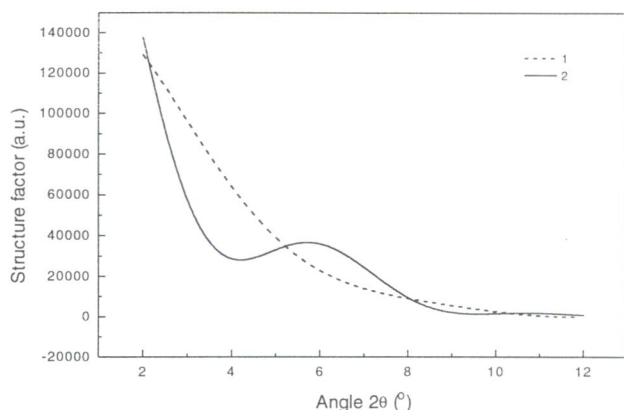


**Fig. 2.** The angular dependences of structure factor for Na-MMT matrix (1), MMT intercalated with gibbsite-type double ring sandwich (2) with the concentration of Al atoms in interlayer per unit cell is 2.66.

Chemical analysis showed 2.66 Al atoms in the interlayer per unit cell which corresponds either to Keggin 5+ ions  $[\text{Al}_{13}\text{O}_4(\text{OH})_{26}(\text{H}_2\text{O})_{10}]^{5+}$  or to gibbsite-type double ring sandwich  $[\text{Al}_{20}(\text{OH})_{54}(\text{H}_2\text{O})_{22}]^{6+}$ . Structure model CERIU<sup>2</sup> computer simulations (Čapková et al.) for both of these structures gave the same d-spacing ( $d_{001} = 19.6 \times 10^{-10}\text{m}$ ) for both of them. The following  $^{27}\text{Al}$  NMR spectroscopy did not prove the tetrahedral Al coordination which is typical for Keggin cations.

## Results and discussion

The above described apparatus (i.e. the correcting functions) was investigated step by step and was then applied to the measured diffractogram of intercalated montmorillonite. Fig. 2 illustrate the angular dependence for the structure factor of natural montmorillonite and montmorillonite intercalated with gibbsite-type double ring sandwich.

In our case of the low angle diffraction ( $2\theta = 2^\circ - 12^\circ$ ) the following specific features of low angle diffraction geometry should be taken into account:

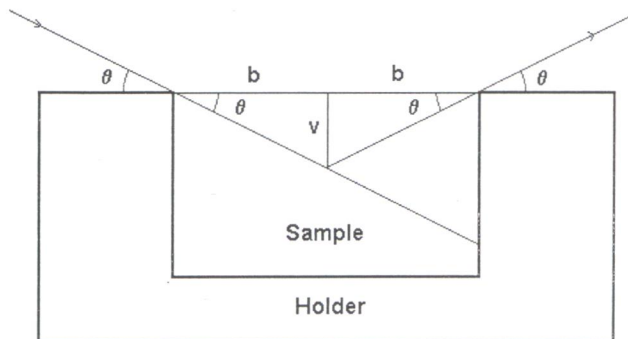


**Fig. 3.** The absorption of sample holder.

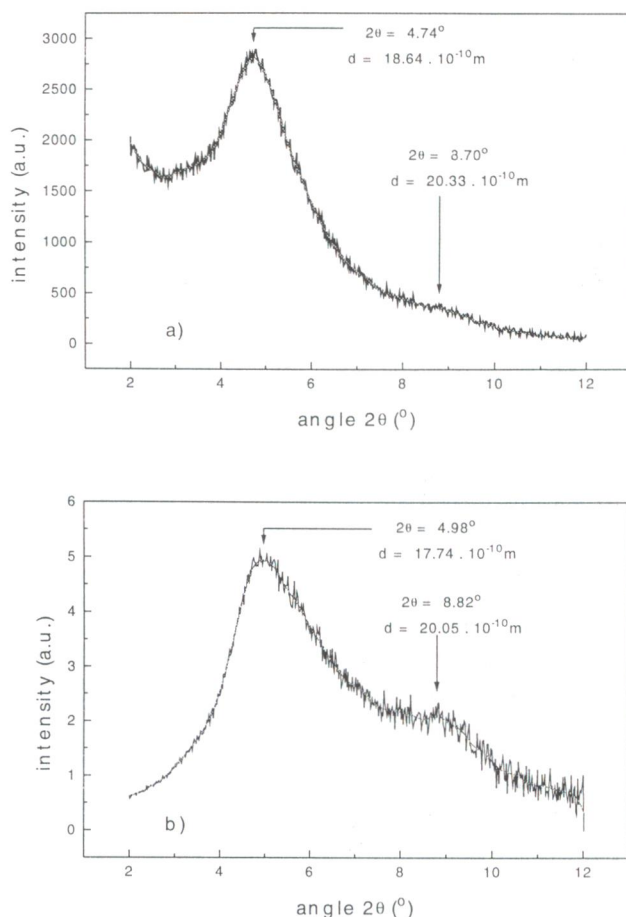


**Fig. 4.** a) measured profile of intercalated MMT (concentration 2.66 Al atoms in interlayer per unit cell, Bragg-Brentano geometry), b) Lorentz polarisation factor corrected profile, the asymmetry of the peak is caused by the Na-MMT matrix peak.

### 1. The absorption of the sample holder

The sample is placed in a plastic holder (see Fig. 3). Part of the diffracted radiation is absorbed by the holder with the result that the irradiated volume is not equal to the volume from which the diffracted radiation is detected. This diffracting volume is for Bragg-Brentano geometry of a shape of prism with trigonal base and is proportional to  $\text{tg}\theta$ .

### 2. The primary beam intensity

According to Bragg-Brentano geometry the trace of the primary beam is not constant but changes with the diffraction angle. The dependence is

$$1/\sin\theta.$$

At low angles the trace of the primary beam is very large, even larger than the area of the sample and part of the primary beam irradiates the sample holder. At higher angles the trace gets smaller and the whole primary beam irradiates only the sample.

The profile analysis of the powder diffractogram of intercalated montmorillonite.

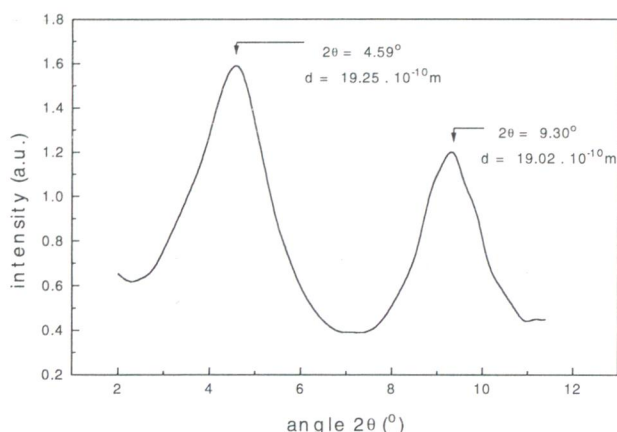


**Fig. 5.** Interference function (measured profile after all corrections) for MMT intercalated with gibbsite-type double ring sandwich, 25% of nonintercalated matrix included in the structure factor.

Using all these corrections together, the detailed profile analysis of intercalated montmorillonite was possible.

The measured diffractogram and the Lorentz-polarization factor corrected diffractogram are given in Fig. 4. There are differences in the  $d$ -spacings of the raw data and the  $L_p$ -corrected data and moreover the (001) and (002)  $d$ -spacings do not match together. This proves that the Lorentz polarization correction is not enough for reliable  $d$ -spacing estimation. In Fig. 4b) the asymmetry of the peak leads to the conclusion that a Na-MMT peak is also present. That is why for higher accuracy 25 % of Na-MMT nonintercalated matrix was included in the structure factor calculation.

Using all of the correcting functions we get the pure interference function shown in Fig. 5.

The line positions after the gibbsite-type double ring sandwich correction agree perfectly with the computer simulations and also the  $d_{001}$  and  $2d_{002}$  are very near to each other (the range of errors was estimated as  $0.20 \times 10^{-10}$  m).

Moreover the line profiles and positions of the interference function agree with the theoretically simulated profiles for Al-MMT ( $d_{001} = 19.5 \times 10^{-10}$  m) and do not fit with line profiles and positions simulated for mixed structure (75 % Al-MMT with  $d_{001} = 19.5 \times 10^{-10}$  m and 25 % Na-MMT with  $d_{001} = 12.5 \times 10^{-10}$  m). Therefore there is no evidence for this sample to be a mixed structure.

## Conclusions

The present result confirmed the fact, that X-ray diffraction profile analysis of clay minerals exhibiting the diffraction line broadening should include the corrections for all the angle dependent factors in intensity formula which can lead to the shift of the peak maxima. Lattice spacings may differ significantly from those corresponding to the raw data or to the  $L_p$  corrected data. In this particular case the misfit between the  $d_{001}$  and  $d_{002}$  is even greater after the  $L_p$  correction than in the raw data. The correction of the diffraction pattern is necessary for a reliable conclusion about the structure.

This profile analysis can also indicate the incorrect model as it was in the case of Keggin cation in the interlayer. This is possible due to different angular dependencies of structure factor.

Our results indicate that both forms — the Al intercalated MMT and the nonintercalated Na-MMT matrix are present in the sample (from chemical analysis) and they do not form a mixed structure (from comparison of measured and simulated interference function).

**Acknowledgment:** This work was supported by the Grant Agency of the Czech Republic (205/94/0468), the Grant Agency of the Charles University (33) and by the US – Czechoslovak Science and Technology Joint Fund Grant No. 93008.

## References

- Berg A.J.v.d., Wachters J.J., private communication.
- Čapková P., Driessen R.A.J., Numan M., Schenk H., Weiss Z. & Klika Z., Simulations: Montmorillonite intercalated with aluminium complex cation. *Chemical Papers*, in print.
- Klug H.P. & Alexander L.E., 1974: X-Ray Diffraction Procedures, John Wiley & Sons, New York.
- Reynolds R.C., 1980: Interstratified Clay Minerals (Chapter 4 in Crystal Structures of Clay Minerals and Their X-ray Identification edited by Brindley G.W., Brown G.), Mineralogical Society, London.
- Reynolds R.C., 1989: Diffraction by Small and Disordered Crystals (Chapter 6 in Modern Powder Diffraction edited by Bish D.L., Post J.E.), The Mineralogical Society of America, Washington, D.C.